Journal of Applied and Computational Mechanics, Vol. 1, No. 3, (2015), 122-133
DOI: 10.22055/jacm.2015.10971

Shahid Chamran University

Journal of
Applied and Computational Mechanics

Size-dependent free vibration analysis of rectangular nanoplates with the consideration of surface effects using finite difference method

Morteza Karimi[1], Mohammad Hossein Shokrani[2], Ali Reza Shahidi[3]

[1]MSc, Department of Mechanical Engineering, Isfahan University of Technology
Isfahan, 84156-83111, Iran, morteza.karimi@me.iut.ac.ir,

[2]MSc, Department of Mechanical Engineering, Isfahan University of Technology
Isfahan, 84156-83111, Iran, mh.shokrani@me.iut.ac.ir,

[3]Assistant Professor, Department of Mechanical Engineering, Isfahan University of Technology
Isfahan, 84156-83111, Iran, shahidi@cc.iut.ac.ir,

Received January 11 2015; revised February 11 2015; accepted for publication February 11 2015.
Corresponding author: Morteza Karimi, morteza.karimi@me.iut.ac.ir

Abstract

In this article, finite difference method (FDM) is used to study the size-dependent free vibration characteristics of rectangular nanoplates considering the surface stress effects. To include the surface effects in the equations, Gurtin-Murdoch continuum elasticity approach has been employed. The effects of surface properties including the surface elasticity, surface residual stress and surface mass density are considered to be the main causes for size-dependent behavior that arise from the increase in surface-to-volume ratios at smaller scales. Numerical results are presented to demonstrate the difference between the natural frequency obtained by considering the surface effects and that obtained without considering surface properties. It is observed that the effects of surface properties tend to diminish in thicker nanoplates, and vice versa.

Keywords: free vibration; surface effects; size-dependent; rectangular nanoplate; finite difference method

1. Introduction

Nanoscience and nanotechnology is now regarded as one of the fastest developing and most revolutionary fields of research, which has sparked promising novel technologies. Nanoscale structures such as nanobeams, nanoplates, nanotubes and nanoparticles, which can be considered as the outcomes of direct molecular manipulation, are the essential building blocks for various types of nanosystems and nanodevices [1, 2]. In recent years, there has been a significant interest in developing micro/nanomechanical and micro/nanoelectromechanical systems (MEMS/NEMS), such as capacitive sensor, switches, actuators, and so on. These devices can be contributed to novel technological developments in many fields leading to industrial revolution [3, 4]. So far, three main methods have been presented for studying mechanical behavior of nanostructures. These include atomistic [5, 6], semi-continuum [7], and classical continuum models [8, 9]. However, both the atomistic and semi-continuum models are computationally expensive and are not suitable for analyzing large-scale systems. Thus, the continuum mechanics approaches are widely preferred due to their simplicity. The main feature of structures is their high surface-to-volume ratio, which makes elastic response of their surface layers to be different from macroscale structures. For this reason, Gurtin and Murdoch [10, 11] developed a theoretical framework based on continuum mechanics concepts that included the effects of surface and interfacial energies. In their approach, the surface was modeled as a mathematical layer of zero thickness perfectly bonded to an underlying bulk substance. The surface (interface) had its own properties, which were different from those of the bulk material. These properties, such as surface energies, affect on physical, mechanical, and electrical properties as well as mechanical response of the nanostructure and can cause interesting behavior. For example, Assadi *et al*. [12] and Assadi [13] studied free and forced vibration of nanoplates considering surface effects. Moreover, Assadi and Farshi [14, 15] investigated surface effects on the vibration and buckling of circular nanoplate. They reported that surface effects could have significant effects on the nanostructures. In addition, increasing in the thickness causes reduction of the surface effects. Gheshlaghi and Hasheminejad [16] and Nazemnezhad *et al*. [17] analyzed surface effects on nonlinear free vibration of nanobeams. Hashemi and Nazemnezhad [18], and Sharabiani and Haeri Yazdi [19] investigated nonlinear free vibrations of functionally graded nanobeams with surface effects. Ansari and Sahmani [20] analyzed bending and buckling behavior of nanobeams by considering surface stress effects and normal stresses, using different beam theories. They indicated that the difference between the behavior of nanobeams predicted with and without surface effects would depend on the magnitudes of the surface elastic constants. Yan and Jiang [21] analyzed the bending and buckling of a thin piezoelectric plate under mechanical and electrical loads, with consideration of surface effects. In these works [12-21], because of using classical solutions, e.g., Navier's method as used for simply-supported boundary conditions, the above-mentioned researchers were not able to study other boundary conditions.

Recently, Ansari *et al*. [22] studied surface energies on the buckling, and maximum deflection of nanoplates using first order shear deformation theory and generalized differential quadrature method (GDQM). Moreover, they [23] analyzed forced vibration of Timoshenko nanobeams based on the surface stress elasticity theory using GDQM. They indicated that the significance of surface effects on the response of nanoplate would rely on its size, type of edge supports, and the selected surface constants. In addition, Farajpour *et al.* [24, 25] studied the surface effects on the axisymmetric buckling and vibration of circular graphene sheets in using differential quadrature method (DQM). They indicated that the size effects would decrease with an increase in the value of surface residual stresses. On the other hand, Mouloodi *et al*. [26, 27] analyzed the surface effects on the bending and vibration of multicrystalline nanoplate. In addition, Wang and Wang [28] investigated the surface effects on the bending and vibration of Mindlin nanoplates. In these works [26-28], the finite element model was used to solve governing equations via classical beam and plate theories. They showed that, depending on the boundary conditions, the deflections and frequencies of nanoplates had a dramatic dependence on the surface effects.

The main objective of this article is to present a numerical method for the investigation of surface effects on the free vibration of rectangular nanoplates with different boundary conditions. Adding the surface effects to the nanoplate's equilibrium equation, makes the equation more complicated. Solving this equation depends on the boundary conditions. If the boundary conditions are simple, the equation will have an analytical solution. However, if the boundary conditions change (e.g., in fixed and free support boundary conditions), numerical methods should be used to solve it. In this paper, first, the governing differential equation has been introduced according to the literature, and then this equation has been solved using the finite difference method (FDM) to obtain the natural frequency for several combinations of boundary conditions. To verify the accuracy of the results obtained by the FDM method, these results have been compared with the results of the analytical approach.

2. Problem statement

Nanoplates are common nanostructures which can be used in the development of NEMS devices such as sensors, actuators and resonators. On the other hand, proper theoretical frameworks are needed to explore and understand the mechanical behavior of nanoplates before they are used in such devices. Moreover, since nanostructures are too small in size, they are always subjected to external actuations by different noise sources. Thus, understanding the dynamic behavior of nanoplates helps the researchers to design proper NEMS devices with lowest noise for different applications. In this article, an attempt has been made to furnish a general framework for the dynamic analysis of nanoplates with the consideration of additional surface properties. Fig. 1 shows a nanoplate with length a, width b, and thickness h. The elasticity modulus, Poisson's ratio and mass density of the bulk part of nanoplate are respectively indicated by E, ν, and ρ. In the present work, λ^s and μ^s are the Lame's surface constants, while τ^s is the surface residual stress which is uniformly distributed on the upper and lower surfaces of the nanoplate. The surface mass density of the nanoplate is also indicated by ρ^s.

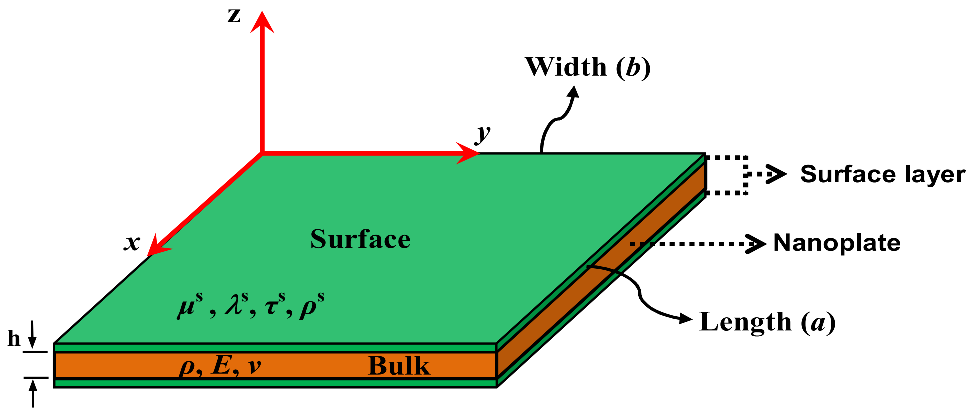

Fig. 1. The geometry of rectangular nanoplate with surface layers

The displacement components in the x, y, and z directions are obtained from the Kirchhoff's plate model, as follows:

$$u_x(x,y,z) = u_0(x,y,t) - z\frac{\partial w(x,y,t)}{\partial x},\ u_y(x,y.z) = v_0(x,y,t) - z\frac{\partial w(x,y,t)}{\partial y},\ u_z(x,y.z) = w(x,y,t) \tag{1}$$

where u_0, v_0, and w are axial and transverse displacements of any point on mid-plane, and t denotes time. Since the axial displacements at the mid-plane (u_0, v_0) have a very small effect, they are neglected for the current analysis. The resulting strain components in Cartesian coordinates, which are always considered to be the same for bulk and surface parts of nanoplates, can be derived from the relations of Eq. (1) as follows:

$$\varepsilon_{xx} = -z\frac{\partial^2 w}{\partial x^2}, \qquad \varepsilon_{yy} = -z\frac{\partial^2 w}{\partial y^2}, \qquad \gamma_{xy} = -2z\frac{\partial^2 w}{\partial x \partial y} \tag{2}$$

Assuming that both nanoplates bulk and surface are homogeneous and isotropic, the stress-strain relation of bulk material subjected to thermal effect are expressed by

$$\begin{Bmatrix} \sigma^b_{xx} \\ \sigma^b_{yy} \\ \sigma^b_{xy} \end{Bmatrix} = \begin{bmatrix} E/(1-\nu^2) & \nu E/(1-\nu^2) & 0 \\ \nu E/(1-\nu^2) & E/(1-\nu^2) & 0 \\ 0 & 0 & G \end{bmatrix} \begin{Bmatrix} \varepsilon_{xx} \\ \varepsilon_{yy} \\ \gamma_{xy} \end{Bmatrix} \tag{3}$$

where E, ν and G denote the elastic modulus, Poisson's ratio and shear modulus, respectively. b is the superscript for bulk properties and effects. The constitutive relations of the surface layers s^+ and s^-, as given by Gurtin and Murdoch [10], can be expressed as

$$\begin{aligned} &\sigma^{s\pm}_{\alpha\beta} = \tau^{s\pm}(\delta_{\alpha\beta} + u_{\alpha,\beta}) + (\mu^{s\pm} - \tau^{s\pm})(u_{\alpha,\beta} + u_{\beta,\alpha}) + (\lambda^{s\pm} + \tau^{s\pm})u_{\gamma,\gamma}\delta_{\alpha\beta}\ ,\ \alpha,\beta,\gamma = x,y \quad (z = \pm\frac{h}{2}) \\ &\sigma^{s\pm}_{\alpha z} = \tau^{s\pm}u_{z,\alpha}\,, \qquad \alpha = x,y \end{aligned} \tag{4}$$

where $\delta_{\alpha\beta}$ is the Kronecker delta and $\alpha=\beta=\gamma=x$, y. $\tau^{s\pm}$ are the residual surface tension components in Newtons per meter under unconstrained conditions, while $\lambda^{s\pm}$ and $\mu^{s\pm}$ are the surface Lame constants on the s^+ and s^- surfaces, respectively. Substituting the strain components from Eq. (2) into Eq. (4) gives additional surface stress components in terms of transverse displacement (w), as follows:

$$\begin{aligned} &\sigma^{s\pm}_{xx} = \tau^s + (2\mu^s + \lambda^s)\varepsilon_{xx} + (\tau^s + \lambda^s)\varepsilon_{yy} = \tau^s \mp \frac{h}{2}(2\mu^s + \lambda^s)\frac{\partial^2 w}{\partial x^2} \mp \frac{h}{2}(\tau^s + \lambda^s)\frac{\partial^2 w}{\partial y^2} \\ &\sigma^{s\pm}_{yy} = \tau^s + (2\mu^s + \lambda^s)\varepsilon_{yy} + (\tau^s + \lambda^s)\varepsilon_{xx} = \tau^s \mp \frac{h}{2}(2\mu^s + \lambda^s)\frac{\partial^2 w}{\partial y^2} \mp \frac{h}{2}(\tau^s + \lambda^s)\frac{\partial^2 w}{\partial x^2} \\ &\sigma^{s\pm}_{xy} = \frac{1}{2}(2\mu^s - \tau^s)\gamma_{xy} = \mp\frac{h}{2}(2\mu^s - \tau^s)\frac{\partial^2 w}{\partial x \partial y} \\ &\sigma^{s\pm}_{xz} = \tau^s\frac{\partial w}{\partial x} \quad , \quad \sigma^{s\pm}_{yz} = \tau^s\frac{\partial w}{\partial y} \end{aligned} \tag{5}$$

The resultant bending moments acting on the cross sections of a nanoplate are obtained by the following integral equations:

$$\begin{aligned} &M_{xx} = (\sigma^{s+}_{xx} - \sigma^{s-}_{xx})\frac{h}{2} + \int_{-h/2}^{h/2} \sigma^b_{xx}\, z dz, \\ &M_{yy} = (\sigma^{s+}_{yy} - \sigma^{s-}_{yy})\frac{h}{2} + \int_{-h/2}^{h/2} \sigma^b_{yy}\, z dz, \\ &M_{xy} = (\sigma^{s+}_{xy} - \sigma^{s-}_{xy})\frac{h}{2} + \int_{-h/2}^{h/2} \sigma^b_{xy}\, z dz. \end{aligned} \tag{6}$$

As can be observed from equations (6), the resultant bending moments acting on the nanoplate's cross sections have two distinct parts: the first part is the contribution of bulk stress components, and the second part arises from surface stresses. Consequently, by substituting equations (5) and (3) into equations (6) and then simplifying the obtained relations, the resultant bending moments with respect to transverse displacement (w) are acquired as follows:

$$M_{xx} = -\left(D + \frac{h^2(2\mu^s + \lambda^s)}{2}\right)\frac{\partial^2 w}{\partial x^2} - \left(\nu D + \frac{h^2(\tau^s + \lambda^s)}{2}\right)\frac{\partial^2 w}{\partial y^2}, \tag{7}$$

$$M_{yy}=-\left(D+\frac{h^2(2\mu^s+\lambda^s)}{2}\frac{\partial^2 w}{\partial y^2}\right)-\left(\nu D+\frac{h^2(\tau^s+\lambda^s)}{2}\right)\frac{\partial^2 w}{\partial x^2},$$

$$M_{xy}=-\left(D(1-\nu)+\frac{h^2(2\mu^s-\tau^s)}{2}\right)\frac{\partial^2 w}{\partial x\partial y}$$

In these equations, D is the classical flexural rigidity of the nanoplate without considering surface effects. Note that the Poisson's ratio of the bulk and surface parts remains the same, since the displacement field over the nanoplate's thickness is considered to be continuous. In order to derive the equilibrium equations of the nanoplate, it would be necessary to find the shear forces acting on the cross sections. Additional cross sectional shear forces, obtained from equations (5) and (4), must be added to the classical terms of shear force resultants. This concept must be considered for both the lower and upper surfaces of the nanoplates, as follows:

$$\begin{aligned} Q_x &= M_{xx,x}+M_{xy,y}+\sigma_{xz}^{s+}+\sigma_{xz}^{s-} \\ Q_y &= M_{yy,y}+M_{xy,x}+\sigma_{yz}^{s+}+\sigma_{yz}^{s-} \end{aligned} \tag{8}$$

The other equilibrium equation for a rectangular nanoplate in the transverse direction has been presented in [13]:

$$Q_x+Q_y=\int_{-h/2}^{h/2}\rho(z)\frac{\partial^2 w}{\partial t^2}dz=(2\rho^s+\rho h)\frac{\partial^2 w}{\partial t^2}. \tag{9}$$

Finally, by substituting equations (8) into Eq. (9) and reformulating the obtained relations, the generalized differential equation for the free vibration of rectangular nanoplates will be derived as a pure function of transverse displacement (w):

$$(D+\frac{h^2(2\mu^s+\lambda^s)}{2})\nabla^4 w-2\tau^s\nabla^2 w=-(2\rho^s+\rho h)\frac{\partial^2 w}{\partial t^2} \tag{10}$$

In Eq. 10, $\nabla^2=(\partial^2/\partial x^2)+(\partial^2/\partial y^2)$ is the Laplacian operator. The vibrations response is harmonic; therefore, the deflection due to vibrations of a thin plate can be expressed as:

$$w(x,y,t)=W(x,y)e^{i\omega t} \tag{11}$$

where ω is the natural frequency and i^2=-1. Substituting Eq. (11) into Eq. (10) yields a biharmonic partial differential equation, involving natural mode $W(x,y)$

$$\begin{aligned} &(D+\frac{h^2(2\mu^s+\lambda^s)}{2})\left(\frac{\partial^4 W}{\partial x^4}+2\frac{\partial^4 W}{\partial x^2\partial y^2}+\frac{\partial^4 W}{\partial y^4}\right) \\ &-2\tau^s\left(\frac{\partial^2 W}{\partial x^2}+\frac{\partial^2 W}{\partial y^2}\right)-\omega^2(2\rho^s+\rho h)W=0 \end{aligned} \tag{12}$$

3. Solution procedure

3.1 Navier's method

Based on the Navier's method, the exact solutions for the free vibration of nanoplates, regarding simply-supported boundary condition are expressed by

$$W=\sum_{m=1}^{\infty}\sum_{n=1}^{\infty}W_{mn}\sin(\alpha x)\sin(\beta y) \tag{13}$$

where $\alpha=m\pi/a$, and $\beta=n\pi/b$. m and n are half-wave number along x and y direction. Substituting Eq. (13) into Eq.(12), the fundamental frequency is obtained:

$$\omega^2=\frac{(D+\frac{h^2(2\mu^s+\lambda^s)}{2})(\alpha^2+\beta^2)^2+2\tau^2(\alpha^2+\beta^2)}{(2\rho^s+\rho h)} \tag{14}$$

3.2 Finite difference method

The finite difference method is a powerful method for solving differential equations. Recently, Karamooz Ravari *et al*. [29, 30] studied nonlocal effect on the buckling of rectangular, circular, and annular nanoplates using finite difference method. The finite difference method replaces the nanoplate differential equation and the expressions defining the boundary conditions with equivalent differences equations. The solution of the bending problem thus reduces to the simultaneous solution of a set of algebraic equations written for every nodal point within the nanoplate. Fig. 2 shows a rectangular nanoplate and the grid points which will be used in the finite difference method. By using this method, Eq. (15) can be used to estimate the derivative of the transverse displacement, W, for the i, j-th point as a function of its neighboring points.

$$\begin{aligned}
&\frac{dW}{dx} = \frac{1}{2r_x}(W_{(i+1,j)} - W_{(i-1,j)}) \\
&\frac{dW}{dy} = \frac{1}{2r_y}(W_{(i,j+1)} - W_{(i,j-1)}) \\
&\frac{d^2W}{dx^2} = \frac{1}{r_x^2}(W_{(i+1,j)} - 2\,W_{(i,j)} + W_{(i-1,j)}) \\
&\frac{d^2W}{dy^2} = \frac{1}{r_y^2}(W_{(i,j+1)} - 2\,W_{(i,j)} + W_{(i,j-1)}) \\
&\frac{d^4W}{dx^4} = \frac{1}{r_x^4}(W_{(i+2,j)} - 4W_{(i+1,j)} + 6\,W_{(i,j)} - 4W_{(i-1,j)} + W_{(i-2,j)}) \\
&\frac{d^4W}{dy^4} = \frac{1}{r_y^4}(W_{(i,j+2)} - 4W_{(i,j+1)} + 6\,W_{(i,j)} - 4W_{(i,j-1)} + W_{(i,j-2)}) \\
&\frac{d^4W}{dx^2dy^2} = \frac{1}{r_x^2 r_y^2}\begin{pmatrix} W_{(i+1,j+1)} + W_{(i-1,j+1)} + W_{(i-1,j-1)} + W_{(i+1,j-1)} + 4W_{(i,j)} \\ -2(W_{(i+1,j)} + W_{(i,j+1)} + W_{(i-1,j)} + W_{(i,j-1)}) \end{pmatrix}
\end{aligned} \tag{15}$$

Here r_x and r_y are the distance between two grid points in the x and y directions, respectively. Substituting Eq. (15) into Eq. (12) and developing a computer code in MATLAB the governing equation are solved.

$$\begin{aligned}
&(D + \frac{h^2(2\mu^s + \lambda^s)}{2})\Bigg\{\frac{1}{r_x^4}\Big(W_{(i+2,j)} - 4W_{(i+1,j)} + 6\,W_{(i,j)} - 4W_{(i-1,j)} + W_{(i-2,j)}\Big) \\
&+ \frac{1}{r_y^4}\Big(W_{(i,j+2)} - 4W_{(i,j+1)} + 6\,W_{(i,j)} - 4W_{(i,j-1)} + W_{(i,j-2)}\Big) \\
&+ \frac{2}{r_x^2 r_y^2}\Big(W_{(i+1,j+1)} + W_{(i-1,j+1)} + W_{(i-1,j-1)} + W_{(i+1,j-1)} + 4W_{(i,j)}\Big) \\
&- \frac{4}{r_x^2 r_y^2}\Big(W_{(i+1,j)} + W_{(i,j+1)} + W_{(i-1,j)} + W_{(i,j-1)}\Big)\Bigg\} - 2\,\tau^s\Bigg\{\frac{1}{r_x^2}\Big(W_{(i+1,j)} - 2\,W_{(i,j)} + W_{(i-1,j)}\Big) \\
&+ \frac{1}{r_y^2}\Big(W_{(i,j+1)} - 2\,W_{(i,j)} + W_{(i,j-1)}\Big)\Bigg\} - \omega^2(2\rho^s + \rho h)\,W_{(i,j)} = 0
\end{aligned} \tag{16}$$

3.3 Boundary conditions

In this article, the free and simply-supported boundary conditions are investigated. Therefore, in this subsection these boundary conditions are introduced, as shown in Fig.3.

3.3.1 Simply-supported boundary conditions

The simply-supported boundary conditions at all edges of nanoplate can be written as:

$$\begin{aligned}
&\frac{\partial^2 W}{\partial x^2} = 0 \\
&\frac{\partial^2 W}{\partial y^2} = 0 \\
&W = 0
\end{aligned} \tag{17}$$

These conditions lead to the following expressions:

$$\begin{aligned}
&W_{(i,j)} = -W_{(i,j+2)},\quad W_{(i,j)} = -W_{(i,j-2)},\quad W_{(i,j+3)} = -W_{(i,j-1)},\quad W_{(i,j-3)} = -W_{(i,j+1)} \\
&W_{(i,j)} = -W_{(i-2,j)},\quad W_{(i,j)} = -W_{(i+2,j)},\quad W_{(i-3,j)} = -W_{(i+1,j)},\quad W_{(i+3,j)} = -W_{(i-1,j)}
\end{aligned} \tag{18}$$

$$W_{(i,j\pm1)} = W_{(i+1,j\pm1)} = W_{(i-1,j\pm1)} = W_{(i\pm1,j)} = 0$$

3.3.2. Free-supported boundary conditions

The free-supported boundary conditions could be expressed as follows:

$$M_x = 0 \qquad V_x = 0 \tag{19}$$

These conditions lead to the following expressions:

$$W_{(i+1,j)} + (-2-2\nu)W_{(i+2,j)} + W_{(i+3,j)} + \nu W_{(i+2,j+1)} + \nu W_{(i+2,j-1)} = 0$$

$$\begin{aligned} &-W_{(i-1,j)} + (\nu-2)W_{(i,j+1)} + (6-2\nu)W_{(i,j)} + (\nu-2)W_{(i,j-1)} + (2-\nu)W_{(i+2,j+1)} + \\ &(2\nu-6)W_{(i+2,j)} + (2-\nu)W_{(i+2,j-1)} + W_{(i+3,j)} = 0 \end{aligned} \tag{20}$$

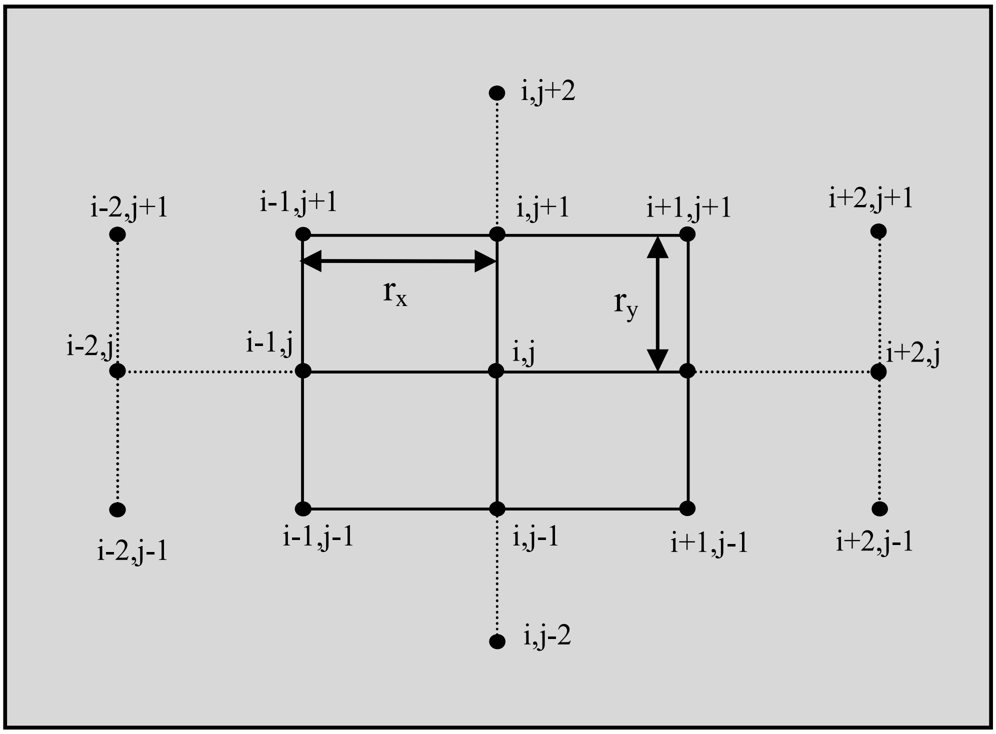

Fig. 2 The rectangular nanoplate and finite difference grid points

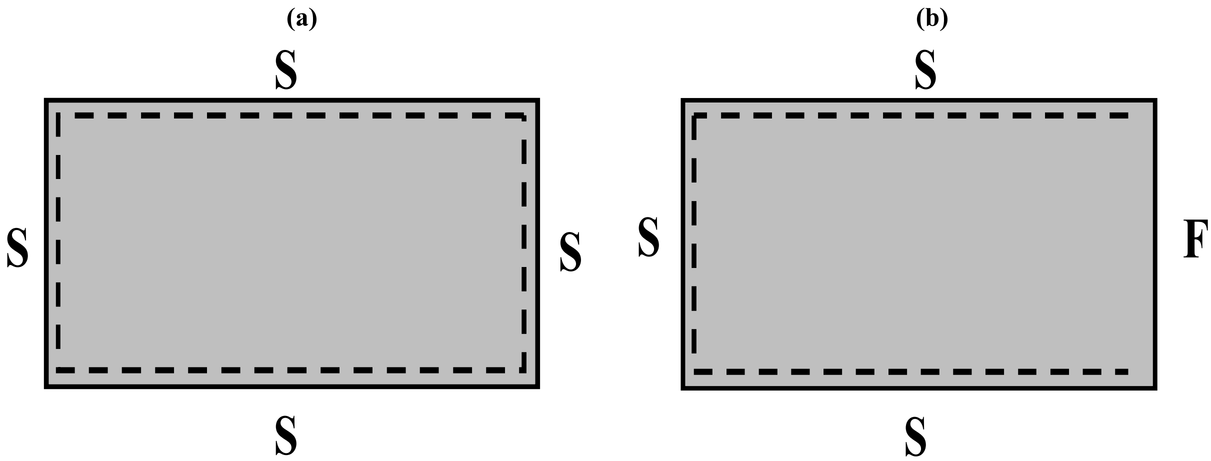

Fig. 3 Combinations of boundary conditions, **(a)** simply-supported, **S**, **(b)** free-supported, **F**.

4. Numerical results and discussion

In this section, we have attempted to illustrate the size-dependent behavior of natural frequencies of rectangular nanoplates. For this purpose, the normalized natural frequencies (NNFs) are depicted in different examples versus the nanoplates' geometric parameters and mode numbers. The NNF is the ratio of the natural frequency obtained with the consideration of surface effects to that obtained without the consideration of surface properties. Consequently, any deviation of NNF from unity indicates the effect of surface properties on the natural frequency. Conversely, as this parameter goes to unity, the effect of surface properties diminishes. The numerical results of this section are given for aluminum nanoplates with the following material properties [13], in which E^s is the surface elasticity:

$$E = 68.5\,Gpa,\quad \nu = \nu^s = 0.35,\quad \rho = 2700\ Kg/m^3,\quad \tau^s = 0.91\,N/m,\quad \rho^s = 5.46e^{-7}\ Kg/m^3$$
$$E^s = 6.09\,N/m,\quad \mu^s = \frac{E^s}{2(1+\nu)} = 2.26\,N/m,\quad \lambda^s = \frac{E^s\nu}{(1+\nu)(1-2\nu)} = 5.26\,N/m \tag{21}$$

Because finite difference method results are sensitive to lower grid points, a convergence test is performed to determine the minimum number of grid points required to obtain stable and accurate results for Eq. (16). In Fig. 4, dimensionless natural frequencies ($\omega a^2\ (\rho h/D)^{0.5}$) is plotted versus the number of grid points for various length of nanoplates. According to Fig. 4, the present solution is converging. From this figure, it is clearly seen that fourteen number of grid points (N=M=14) are sufficient to obtain the accurate solutions for the vibration analyses.

For the first numerical example, the NNF is evaluated for different combinations of nanoplates' length (a), thickness (h) and vibration mode shape (m). Figs 5(a) and 5(b) show the effect of thickness on NNF of square nanoplates no different nanoplates length with simply and free-supported boundary conditions, respectively. It is concluded from the numerical results in Figs. 5(a) and 5(b) that as a nanoplate gets thicker, the effects of surface properties tend to diminish, and vice versa. However, the curves of Figs. 5(a) and 5(b) get closer to each other at higher values of length, so that for a >100 nm and a >120 nm, the NNF becomes more saturated as length increases. This means that the NNF is more sensitive to nanoplate length at smaller scales.

Figs 6(a) and 6(b) indicate the effect of length on NNF of square nanoplates for different vibration mode numbers, m, with simply and free-supported boundary conditions, respectively. From Figs. 6(a) and 6(b), it is observed that the effect of surface properties can be ignored at higher modes of vibration. It should also be mentioned that the NNF decreases considerably from vibration mode I to mode II; while this is not seen at higher modes where the corresponding curves converge to each other at m >4 and m >5, respectively.

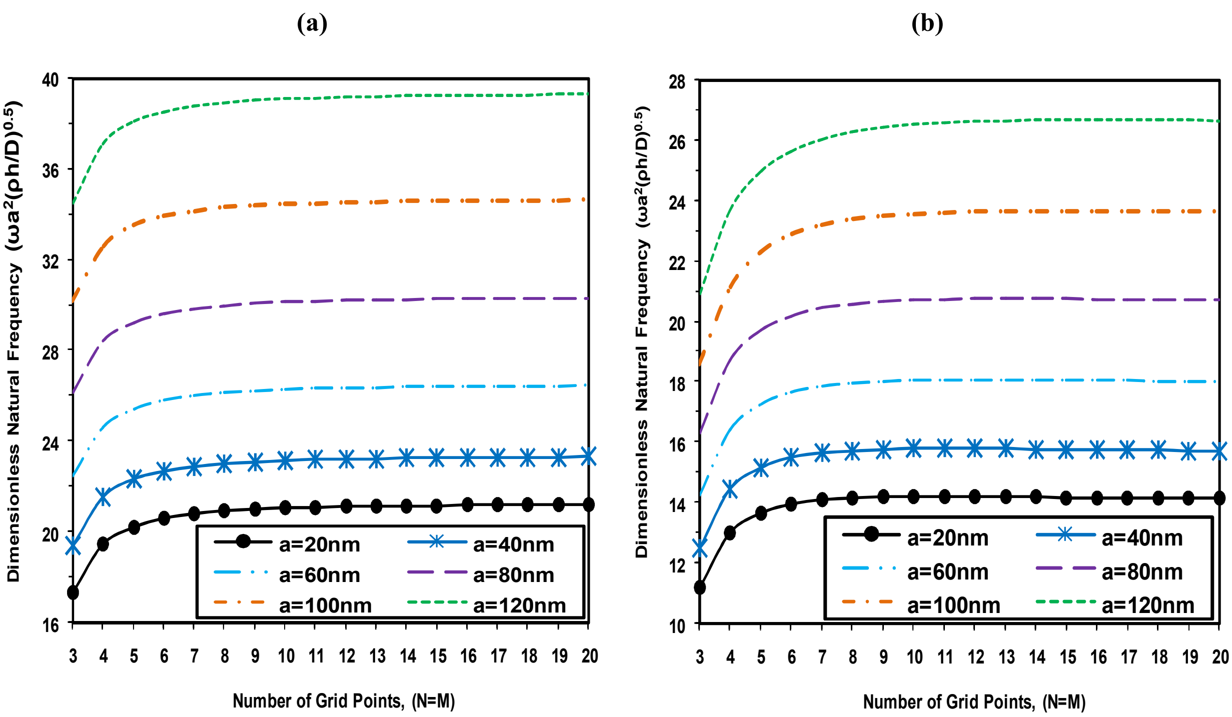

Fig. 4 Convergence study and minimum number of grid points required for obtaining accurate results for dimensionless natural frequencies by finite difference method with various nanoplate length, (h=4 nm), **(a)** simply-support boundary conditions, **(b)** free-support boundary conditions.

(a) (b)

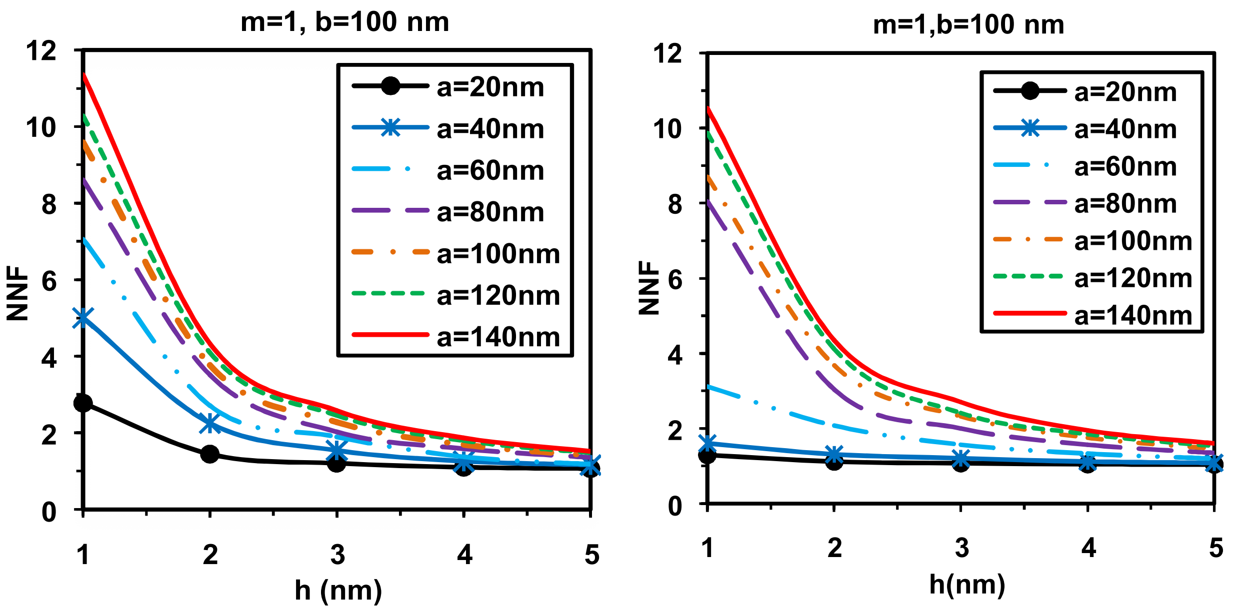

Fig. 5 The NNF of nanoplates versus thickness for various nanoplate length **(a)** simply-supported boundary conditions, **(b)** free-supported boundary conditions.

(a) (b)

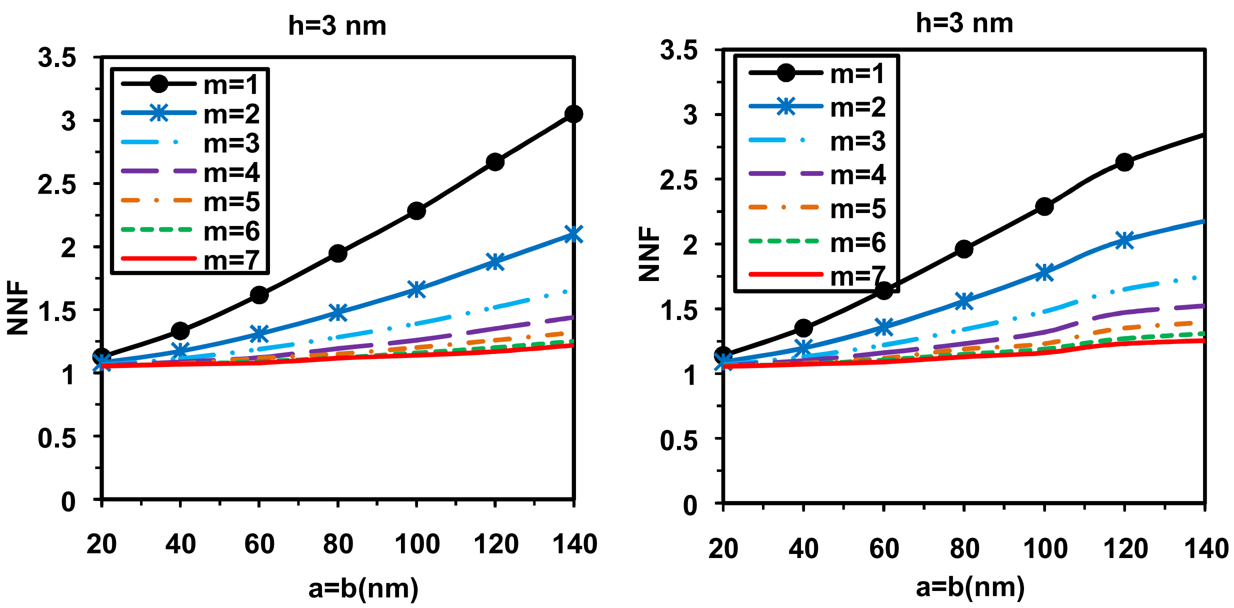

Fig. 6 The NNF of nanoplates versus length for various frequency number, *m*, **(a)** simply-supported boundary conditions, **(b)** free-supported boundary conditions.

Table 1 Ratios of ω_m/ω_1 for aluminum nanoplates with simply-supported boundary conditions (h=2 nm)

		a=100 *nm*					*a*=50 *nm*				
η		m=1	2	3	4	5	m=1	2	3	4	5
1	FDM	1	1.66	2.52	3.54	4.79	1	1.85	3.12	4.76	6.85
	Exact	1	1.66	2.52	3.57	4.83	1	1.83	3.07	4.76	6.90
0.5	FDM	1	1.28	1.65	2.01	2.60	1	1.33	1.79	2.39	3.12
	Exact	1	1.28	1.66	2.12	2.64	1	1.32	1.79	2.41	3.16

Table 2 Ratios of ω_m/ω_1 for aluminum nanoplates with simply-supported boundary conditions (*h*=4 *nm*)

η		*a*=100 *nm*					*a*=50 *nm*				
		m=1	2	3	4	5	m=1	2	3	4	5
1	FDM	1	1.96	3.46	5.42	7.99	1	2.25	4.26	6.99	10.81
	Exact	1	1.94	3.43	5.48	8.11	1	2.24	4.29	7.16	10.85
0.5	FDM	1	1.37	1.92	2.63	3.48	1	1.47	2.21	3.23	4.59
	Exact	1	1.36	1.89	2.63	3.54	1	1.46	2.22	3.27	4.62

Table 3 Ratios of ω_m/ω_1 for aluminum nanoplates with free-supported boundary conditions

η	*a* (*nm*)	*h*=2 *nm*					*h*=4 *nm*				
		m=1	2	3	4	5	m=1	2	3	4	5
1	**100**	1	1.65	2.70	3.52	4.11	1	1.75	3.25	4.66	5.62
	50	1	1.69	3.04	4.24	5.05	1	1.95	3.94	5.78	7.10
0.5	**100**	1	3.12	5.21	6.76	9.88	1	2.4	3.00	4.40	6.44
	50	1	2.53	3.24	4.50	6.60	1	2.29	2.94	4.53	6.85

Tables 1 and 2 respectively show the numerical results of ω_m/ω_1 for aluminum nanoplates with thicknesses of h=2 *nm* and h=4 *nm* and simply-supported boundary conditions, and for different modes of vibration, two different side lengths, a, and two different aspect ratios, $\eta=a/b$. Table 3 shows the numerical results of ω_m/ω_1 for aluminum nanoplates with free-supported boundary conditions. From Tables 1 and 2, good agreements can be observed between the FDM results and the results in [13]. The results in [13] are based on an exact analytical solution. Thus, the results in Table 3 can be reliable.

The results of Tables 1 and 2 indicate that for thicker nanoplates, the surface effects are significantly smaller. It is concluded from these tables that ratio ω_m/ω_1 decreases when surface effects are considered. Similarly, it can be observed that at greater surface effects (for example, in thinner and larger nanoplates) the natural frequencies corresponding to different modes of vibration are compacted into a narrower spectrum.

In Table 3, these results hold true for η=1; however, inconsistent results are obtained for η=0.5. For a better understanding of the given results, the diagrams of ω_m/ω_1 ratios versus vibration mode numbers have been presented in Figs. 7 and 8. In Figs. 7 and 8(a), it is observed that in the presence of surface effects, the frequency ratio ω_m/ω_1 becomes even *1/3* or *1/2* of its corresponding classical value. Moreover, it can be seen that the frequency ratio ω_m/ω_1 for all curves with surface effects are lower than curves classical. In contrast, in Fig. 8(b), the frequency ratio ω_m/ω_1 for curve with a=100 nm and h=2 nm, is higher than curve classical. It should be noted here that in the absence of surface effects, the ω_m/ω_1 ratio from the classical plate theory has a unique value for a given η. This has been shown in Figs. 7 and 8 by dotted curves for the corresponding values of η.

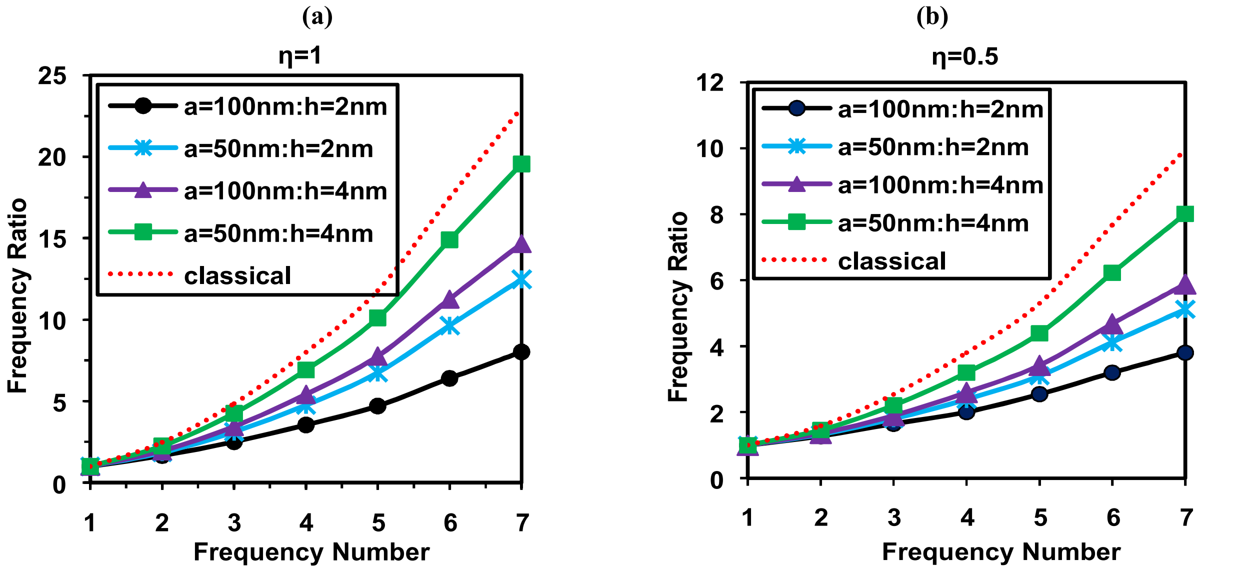

Fig. 7 The ω_m/ω_1 ratios of simply-supported nanoplates versus frequency number, m, for different geometries, **(a)** η=1, **(b)** η=0.5.

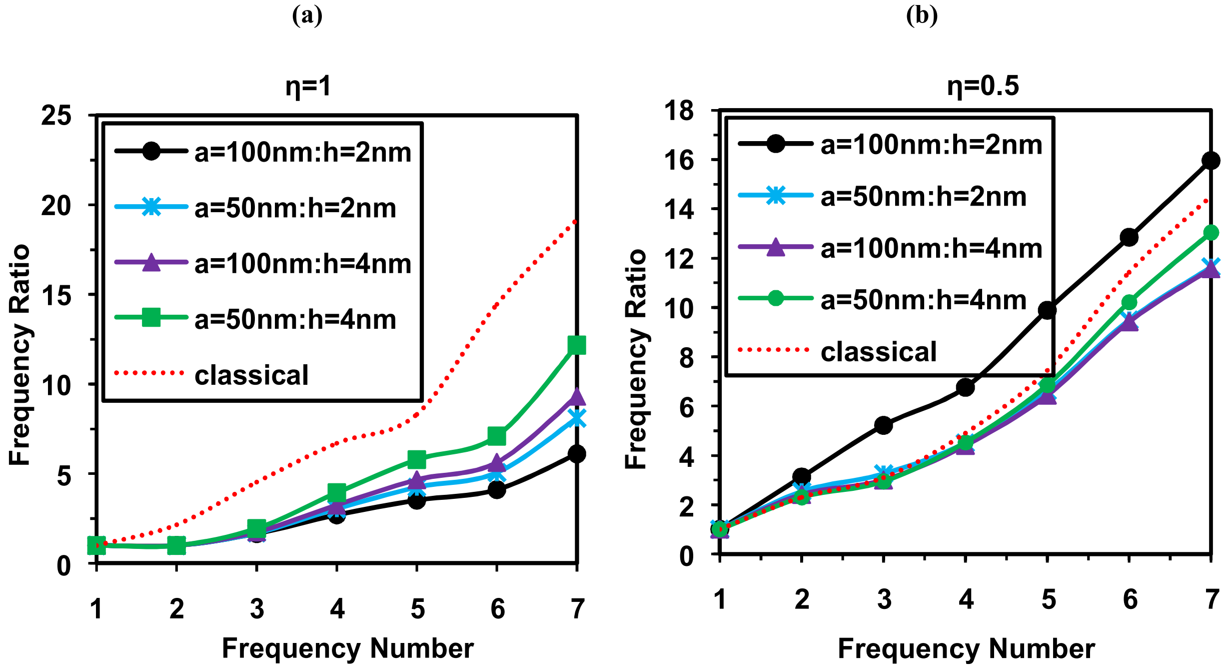

Fig. 7 The ω_m/ω_1 ratios of free-supported nanoplates versus frequency number, *m*, for different geometries, **(a)** η=1, **(b)** η=0.5.

Table 4 Classical ratios of ω_m/ω_1 for aluminum nanoplates (for h=2 *nm* and h=4 *nm*).

		Simply-supported boundary conditions					Free-supported boundary conditions				
η	***a* (*nm*)**	**m=1**	**2**	**3**	**4**	**5**	**m=1**	**2**	**3**	**4**	**5**
1	**100**	1	2.47	4.85	8.01	11.78	1	2.15	4.52	6.70	8.30
	50	1	2.47	4.85	8.01	11.78	1	2.15	4.52	6.70	8.30
0.5	**100**	1	1.59	2.54	3.80	5.30	1	2.30	3.10	4.90	7.45
	50	1	1.59	2.54	3.80	5.30	1	2.30	3.10	4.90	7.45

Table 4 shows the classical numerical results of ω_m/ω_1 for free and simply-supported aluminum nanoplates. It is understood from Table 4 that at a certain value of η, the classical ratio of ω_m/ω_1 is the same for different values of '*a*' and '*h*'. This notion indicates the size-dependent behavior of natural frequencies.

5. Concluding remark

In this study, the size-dependent free vibration of rectangular nanoplates under the effect of additional surface properties for free and simply-supported boundary conditions was studied. FDM was used to solve governing equation. In this method, a complete set of numerical results are given for the NNF of Aluminum nanoplates. The general observation is that as nanoplates get thinner and larger, the effects of surface properties increase. It is also observed that by improving mode numbers (*m*), the surface effects diminish. In the same way, the natural frequencies increase. This finding is more valid for larger nanoplates. It is observed that in some cases the ratio of ω_m/ω_1 for simply and free-supported boundary conditions become even *1/2* or *1/3* of its corresponding classical ratio (where the surface effects had not been considered).

Nomenclature

E	Modulus of elasticity	ε_{ij}	Strain components
E^s	Surface elastic modulus	σ_{ij}^s	Surface stress components
ν	Poisson's ratio	σ_{ij}^b	Bulk stress components
ρ	Mass density	M_{ij}	Bending moment components
ρ^s	Surface mass density	D	Flexural rigidity
τ^s	Surface residual stress	m	Vibration mode shape
λ^s, μ^s	Surface Lame constants	x,y,z	Cartesian coordinates
ω	Natural frequency of nanoplate	r_x, r_y	Distance between two grid points in the x and y directions, respectively

u, v, w	Displacements in the x, y and z directions, respectively	a, b, h	Length, width and thickness of nanoplate, respectively
Superscripts		**Subscripts**	
$( )^{+}$, $( )^{-}$	Upper and lower surfaces of nanoplate, respectively	$( )_{,x}$, $( )_{,y}$	Partial derivatives with respect to x and y, respectively
$( )^{s}$	Surface of nanoplate		

References

[1] Lian, P., Zhu, X., Liang, S., Li, Z., Yang, W., Wang, H., "Large reversible capacity of high quality graphene sheets as an anode material for lithium-ion batteries", Electrochimica Acta, Vol. 55, No. 12, pp. 3909-3914, 2010.

[2] Saito, Y., Uemura, S., "Field emission from carbon nanotubes and its application to electron sources", Carbon, Vol. 38, No. 2, pp. 169-182, 2000.

[3] Sakhaee-Pour, A., Ahmadian, M. T., Vafai, A., "Applications of single-layered graphene sheets as mass sensors and atomistic dust detectors", Solid State Communications, Vol. 145, No. 4, pp. 168-172, 2008.

[4] Wang, Z. L., Song, J., "Piezoelectric nanogenerators based on zinc oxide nanowire arrays", Science, Vol. 312, No. 5771, pp. 242–246, 2006.

[5] Ball, P., "Roll up for the revolution", Nature, Vol. 414, No. 6860, pp. 142–144, 2001.

[6] Baughman, R. H., Zakhidov, A. A., DeHeer, W. A., "Carbon nanotubes–the route toward applications", Science, Vol. 297, No. 5582, pp. 787–792, 2002.

[7] Li, C., Chou, T. W., "A structural mechanics approach for the analysis of carbon nanotubes", International Journal of Solids and Structures, Vol. 40, No. 10, pp. 2487–2499, 2003.

[8] Govindjee, S., Sackman, J. L., "On the use of continuum mechanics to estimate the properties of nanotubes", Solid State Communications, Vol. 110, No. 4, pp. 227–230, 1999.

[9] He, X. Q., Kitipornchai, S., Liew, K. M., "Buckling analysis of multi-walled carbon nanotubes: a continuum model accounting for van der Waals interaction", Journal of Mechanics and Physics of solids, Vol. 53, No. 2, pp. 303–326, 2005.

[10] Gurtin, M. E., Murdoch, A. I., "A continuum theory of elastic material surfaces", Archive for Rational Mechanics and Analysis, Vol. 57, No. 4, pp. 291–323, 1975.

[11] Gurtin, M. E, Murdoch, A. I., "Surface stress in solids", International Journal of Solids and Structures, Vol. 14, No. 4, pp. 431–440, 1978.

[12] Assadi, A., Farshi, B., Alinia-Ziazi, A., "Size dependent dynamic analysis of nanoplates", Journal of Applied Physics, Vol. 107, No. 12, pp. 124310, 2010.

[13] Assadi, A., "Size dependent forced vibration of nanoplates with consideration of surface effects", Applied Mathematical Modelling, Vol. 37, No. 5, pp. 3575–3588, 2013.

[14] Assadi, A., Farshi, B., "Vibration characteristics of circular nanoplates", Journal of Applied Physics, Vol. 108, No. 7, pp. 074312, 2010.

[15] Assadi, A., Farshi, B., "Size dependent stability analysis of circular ultrathin films in elastic medium with consideration of surface energies", Physica E, Vol. 43, No. 5, pp. 1111–1117, 2011.

[16] Gheshlaghi, B., Hasheminejad, S. M., "Surface effects on nonlinear free vibration of nanobeams", Composites Part B: Engineering, Vol. 42, No. 4, pp. 934–937, 2011.

[17] Nazemnezhad, R., Salimi, M., Hosseini Hashemi, S. h., Asgharifard Sharabiani, P., "An analytical study on the nonlinear free vibration of nanoscale beams incorporating surface density effects", Composites Part B: Engineering, Vol. 43, No. 8, pp. 2893–2897, 2012.

[18] Hosseini-Hashemi, S., Nazemnezhad, R., "An analytical study on the nonlinear free vibration of functionally graded nanobeams incorporating surface effects", Composites Part B: Engineering, Vol. 52, pp. 199–206, 2013.

[19] Asgharifard Sharabiani, P., Haeri Yazdi, M. R., "Nonlinear free vibrations of functionally graded nanobeams with surface effects", Composites Part B: Engineering, Vol. 45, No. 1, pp. 581–586, 2013.

[20] Ansari, R., Sahmani, S., "Bending behavior and buckling of nanobeams including surface stress effects corresponding to different beam theories", International Journal of Engineering Science, Vol. 49, No. 11, pp. 1244–1255, 2011.

[21] Yan, Z., Jiang, L., "Surface effects on the electroelastic responses of a thin piezoelectric plate with nanoscale thickness", Journal of Physics D: Applied Physics, Vol. 45, No. 25, pp. 255401, 2012.

[22] Ansari, R., Shahabodini, A., Shojaei, M. F., Mohammadi, V., Gholami, R., "On the bending and buckling behaviors of Mindlin nanoplates considering surface energies", Physica E, Vol. 57, pp. 126–137, 2014.

[23] Ansari, R., Mohammadi, V., Faghih Shojaei, M., Gholami, R., Sahmani, S., "On the forced vibration analysis of Timoshenko nanobeams based on the surface stress elasticity theory", Composites Part B: Engineering, Vol. 60, pp. 158–166, 2014.

[24] Farajpour, A., Dehghany, M., Shahidi, A. R., "Surface and nonlocal effects on the axisymmetric buckling of circular graphene sheets in thermal environment", Composites Part B: Engineering, Vol. 50, pp. 333–343, 2013.

[25] Asemi, S. R., Farajpour, A., "Decoupling the nonlocal elasticity equations for thermo-mechanical vibration of circular graphene sheets including surface effects", Physica E, Vol. 60, pp. 80–90, 2014.

[26] Mouloodi, S., Khojasteh, J., Salehi, M., Mohebbi, S., “Size dependent free vibration analysis of Multicrystalline nanoplates by considering surface effects as well as interface region”, International Journal of Mechanical Sciences, Vol. 85, pp. 160–167, 2014.
[27] Mouloodi, S., Mohebbi, S., Khojasteh, J., Salehi, M., “Size-dependent static characteristics of multicrystalline nanoplates by considering surface effects”, International Journal of Mechanical Sciences, Vol. 79, pp. 162–167, 2014.
[28] Wang, K. F., Wang, B. L., “A finite element model for the bending and vibration of nanoscale plates with surface effect”, Finite Elements in Analysis and Design, Vol. 74, pp. 22–29, 2013.
[29] Karamooz Ravari, M. R., Talebi, S. A., Shahidi, R., “Analysis of the buckling of rectangular nanoplates by use of finite-difference method”, Meccanica Vol. 49, No. 6, pp. 1443–1455, 2014.
[30] Karamooz Ravari, M.R., Shahidi, R., “Axisymmetric buckling of the circular annular nanoplates using finite difference method”, Meccanica Vol. 48, No. 1, pp. 135–144, 2013.